Published in final edited form as:
J Mol Biol. 2008 September 26; 382(1): 213–222. doi:10.1016/j.jmb.2008.06.075.

Subnanometer-resolution Structures of the Grass Carp Reovirus Core and Virion

Lingpeng Cheng[1,2], **Qin Fang**[3,#], **Sanket Shah**[2], **Ivo C. Atanasov**[1], and **Z. Hong Zhou**[1,2,#]

[1]Department of Microbiology, Immunology & Molecular Genetics and the California NanoSystems Institute, The University of California at Los Angeles, 237 BSRB, 615 Charles E. Young Dr. S., Los Angeles, CA 90095-7364, USA

[2]Department of Pathology and Laboratory Medicine, University of Texas Medical School at Houston, Houston, TX 77030

[3]State Key Laboratory of Virology, Wuhan Institute of Virology, Chinese Academy of Sciences; Wuhan, 430071, China

Summary

Grass carp reovirus (GCRV) is a member of the *Aquareovirus* genus of the family *Reoviridae*, a large family of dsRNA viruses infecting plants, insects, fishes and mammals. We report the first subnanometer-resolution three-dimensional (3D) structures of both GCRV core and virion by cryo-electron microscopy (cryoEM). These structures have allowed the delineation of interactions among the over 1000 molecules in this enormous macromolecular machine, and a detail comparison with other dsRNA viruses at the secondary structure level. The GCRV core structure shows that the inner proteins have strong structural similarities even at the level of secondary structure elements with those of orthoreoviruses, indicating that the structures involved in viral dsRNA interaction and transcription are highly conserved. In contrast, the level of similarity in structures decreases in the proteins situated in the outer layers of the virion. The proteins involved in host recognition and attachment exhibit the least similarities to other members of *Reoviridae*. Furthermore, in GCRV, the RNA-translocating turrets are in an open state and lack a counterpart for the σ1 protein situated on top of the close turrets observed in mammalian orthoreovirus (MRV). Interestingly, the distribution and organization of GCRV core proteins resembles those of the cytoplasmic polyhedrosis virus (CPV), a cypovirus and the structurally simplest member of the *Reoviridae* family. Our results suggest that GCRV occupies a unique structure niche between the simpler cypoviruses and the considerably more complex MRV, thus providing an important model for understanding the structural and functional conservation and diversity of this enormous family of dsRNA viruses.

Keywords

Grass carp reovirus; aquareovirus; dsRNA virus; 3D structure; *Reoviridae*; subnanometer-resolution; cryo-electron microscopy; evolution; divergence

[#]***Corresponding authors:*** Phone: 310-983-1033; Fax: (310) 206-5365, Hong.Zhou@UCLA.edu and qfang@wh.iov.cn.

Data deposition and Accession Numbers

Electron density maps have been deposited in the Protein Data Bank and EBI under accession codes XXXX and XXXX.

Introduction

Reoviridae is one of the largest families of viruses and comprises at least 12 genera of viruses with segmented dsRNA genomes.[1; 2] These viruses are enormous macromolecular machines with the remarkable ability of endogenous RNA transcription either *in vivo*, inside the host cytoplasm, or *in vitro*, in a cell-free environment. Despite having a highly conserved and characteristic endogenous transcription mechanism, viruses in this family infect a wide variety of organisms, including mammals, lower vertebrates and invertebrates, and even plants. Genus *Aquareovirus* of the *Reoviridae* family consists of viruses that mainly infect aquatic animals such as bony fish and shellfish isolated from both sea and freshwater origins.[3] Some *Aquareovirus* isolates can lead to severe epidemic hemorrhagic disease and pancreatitis in fish, although the majority has been isolated from seemingly healthy finfish and shellfish.[4] Grass carp reovirus (GCRV), which is considered to be the most pathogenic aquareovirus, was first identified from a breakout of hemorrhage disease affecting a vast majority (~85%) of fingerling and yearling grass carp from southern China.[5] Due to its virulence, GCRV serves as a suitable model for studying the replication and pathogenesis of aquareoviruses in general.

Like most other members of *Reoviridae*, GCRV is a multilayer spherical particle with a diameter of about 800 Å enclosing a dsRNA genome of eleven segments.[6] The virus replicates well in the CIK (*Ctenopharyngodon idellus* kidney) cell line at 25 − 30°C and produces a typical cytopathic effect consisting of large syncytia in its sensitive cells. In addition, the virions are very robust as they are resistant to both chloroform and ether, and remain infectious between pH 3–10 and at high temperatures.[7; 8] Serological analyses indicated that GCRV does not have any antigenic relationship to human rotaviruses and reoviruses, with the exception of a very weak agglutinating reaction observed during a hemagglutination test with human type O blood cells.[9] Six or seven established sub-genogroups (Aquareovirus A–F and/or G) comprising more than 50 different isolates have been identified among the aquareovirus isolates by dsRNA genome electrophoresis and correlated RNA hybridization, as well as antigenic property analyses.[5; 6] Among them, GCRV and striped bass reovirus (SBRV, *Aquareovirus* A) have been characterized the best.[10; 11] Sequence and phylogenic analyses indicated a relatively higher level of sequence homology between aquareoviruses and mammalian orthoreoviruses (MRV) as compared to other members of the family.[10;12]

Many viruses in the family *Reoviridae* have been subjected to extensive three-dimensional (3D) structural analyses -- sometimes up to atomic resolution --by X-ray crystallography and single particle cryo-electron microscopy (cryoEM). Examples include members of the genera *Orthoreovirus*,[13; 14; 15] *Rotavirus*,[16] *Orbivirus*[17] and *Cypovirus*[18] *etc*. In contrast, structures of aquareoviruses have been determined only to about 20-Å resolution.[11; 19; 20] As a result, a definitive structural comparison at the secondary structure level of aquareovirus with viruses in other genera is lacking and the issue of its classification remain controversial.[12;21]

To fill in the missing structural information gap regarding the aquareovirus genus at a resolution sufficient for comparison of protein folds, we have determined the 3D structures of the GCRV core and virion at sub-nanometer resolution by single particle cryoEM reconstruction. The structure of GCRV core shows that the proteins on the innermost layer bear strong structural similarities to those of MRV even at the level of secondary structures and 3D folds, indicating that, as expected, the proteins involved in viral dsRNA interaction and transcription are highly conserved across different genera. However, the attachment of VP6 clamping protein to this innermost layer is different from that in MRV, but is the same as in the cytoplasmic polyhedrosis virus (CPV), a cypovirus and the structurally simplest member of the *Reoviridae* family. Beyond the core, GCRV begins differentiating itself in protein compositions and in domain structures of homolog proteins and shows significant divergence from those of other *Reoviridae* members. Thus, viral proteins involved in host interactions

have evolved significantly in their structures. The structural data clearly suggests that GCRV occupies a unique structural niche when compared to other well studies members of the *Reoviridae* and serves as an important model system for understanding the diversity and conservation of this enormous family of dsRNA viruses.

Results

CryoEM of GCRV inner cores and virions

One of the challenges in structural studies of aquareoviruses is the difficulty in deciphering molecular interactions among the large number of structural proteins making up the inner and outer capsid shells.[11; 19; 20] In order to eliminate ambiguities in resolving molecular boundaries between the inner and outer shell capsid proteins of GCRV, we imaged both the double-shelled, GCRV virions and the simpler, single-shelled GCRV inner core particles; and determined their structures to subnanometer resolution independently. Figure 1A and 1B show representative cryoEM CCD image frames of the frozen hydrated GCRV core and intact virion particles, respectively. The core particles are 810 Å in diameter, when including the turret projections at its fivefold vertices (arrowhead in Fig. 1A), and ~610 Å excluding them (Fig. 1A). Each virion particle is ~880 Å in diameter. A well defined electron lucent boundary divides the virion capsid into an inner and an outer layer (arrow in Fig. 1B). The 3D reconstructions of the core and intact virion were reconstructed from 3697 and 2755 particles, respectively. The effective resolution of both maps was ~9 Å based on the 0.5 cutoff of Fourier shell correlation coefficient between independent reconstructions. To our best knowledge, the subnanometer-resolution reconstructions clearly revealed helices and β sheets, thus allowing a detailed structural description of all five aquareovirus capsid proteins and their interactions at secondary structure level for the first time.

Overall 3D structures of the GCRV core and virion

The shaded surface view of GCRV core structure shows a T=1 capsid shell of 810 Å in diameter, with twelve prominent flower-like turrets on the twelve icosahedral fivefold vertices and 120 less prominent surface protrusions decorating the twenty icosahedral facets (Fig. 2A). The GCRV core is composed of 5 proteins: VP1, VP2, VP3, VP4 and VP6, which, based on amino-acid sequence analyses, are homologs to λ2, λ3, λ1, μ2 and σ2 of MRV, respectively.[11; 19] VP3 forms the continuous capsid shell, which is clamped together by 120 protruding VP6 molecules (green in Fig. 2A). Similar organization (Fig. 2B) is observed in CPV,[18; 22; 23] a member of the *Cypovirus* genus24 of the *Reoviridae*. On each fivefold vertex is a characteristic turret structure, which is a pentamer of VP1 (Fig. 2A).

Beneath each turret is a strong density attributable to the GCRV transcriptase complex, likely a heterologous complex containing RNA-dependent RNA polymerase (VP2) and its putative cofactor/nucleoside triphosphate phosphohydrolase (VP4) (Fig. 2C). The transcriptase complex structures were not resolved clearly, probably due to their partial and/or asymmetric occupancy of the icosahedrally related binding sites underneath the 12 vertices within each GCRV core[14; 25] and are not described further below.

The GCRV virion has an incomplete T=13 icosahedral symmetry, with an overall structural organization identical to those of MRV and avian orthoreovirus (ARV) (Fig. 2D, F).[26; 27] In addition to all the structures present in the inner core, each GCRV virion contains 200 trimers formed by VP5-VP7 heterodimers, a structure that is analogous to the μ1σ3 complex of MRV.[28] These trimers and pentamer proteins VP1 associate one another to form three types of conduits/openings perforating the outer capsid layer:[29] P1, P2 and P3 (Fig. 2D). Similar to ARV, but unlike that in MRV, the inner capsid protein density (yellow) is visible through all the conduits (Fig. 2D). This indicates that GCRV lacks the counterpart densities corresponding

to the C-terminals of μ1 proteins, which were observed to form hub-and-spoke structures in the interior of P2 and P3 conduits of MRV.[15] In addition, unlike closed turret in MRV, the GCRV VP1 turret is open in both the core (Fig. 2A) and the virion (P1 in Fig. 2D). The lack of an MRV σ1 protein homolog (or σC of ARV) [26] in GCRV may account for the open turret structure we observed.

The inner capsid shell protein, VP3

A total of 120 VP3 molecules form the spherical inner capsid shell of the GCRV inner core. Our density map of the VP3 inner shell shows a high degree of structural similarity to MRV λ1, which both demonstrates the validity of our cryoEM reconstruction and confirms a close evolutionary relationship between the two viruses (Fig. 3A). Like corresponding proteins of other *Reoviridae* members, two slightly different conformers of VP3 exist on the capsid shell: VP3A and VP3B (Fig. 2F). Both conformers of VP3 have a plate-like structure with three domains: apical, carapace, and dimerization domains (Fig. 3A), named after nomenclature established for bluetongue virus (BTV) VP3.17 Equivalent framework and general domains in inner capsid proteins have also been identified in other dsRNA viruses other than BTV such as the orthoreovirus core,13 rice dwarf virus (RDV)30 and CPV.18

A direct comparison of our VP3 map with a simulated density map of MRV λ1 (Fig. 3B) indicates that most of the secondary structure elements overlap and are thus highly conserved structurally. Almost all of the α-helices of MRV protein λ1 fit well with the density map of protein VP3 (Fig. 3C, D and E), except for the N-terminal α-helix of MRV λ1 (green helix in Fig. 3C, E). This helix is located in the inner surface facing the viral RNA genome, suggesting that the two viruses may have different RNA organizations inside the capsid proteins.

The turret protein, VP1

Five VP1 molecules (the MRV λ2 protein) comprise a turret, a cylindrical pentameric complex that sits on top of each of the 12 fivefold vertices (Fig. 2A).11 VP1 has been shown to have GTase activity 31 and is also believed to have RNA capping activities with SAM (S-adenosyl-L-methionin) binding domains, similar to the MRV λ2.10; 12 The sequence prediction and structural comparison with λ2 in MRV suggests that the GCRV VP1 turret structure can be divided into a GTase domain, two methylase domains, and an immunoglobulin (Ig)-like flap domain. The locations of these domains are all identified in our VP1 structure (Fig. 3F). The most significant difference was observed in the Ig-like flap domain (marked in Fig 3F). Fitting of the crystal structure of the λ2 protein into our density map of VP1 revealed that the Ig-like flap domain is tilted away from the fivefold axis, resulting in an open channel in GCRV turret (Fig. 2A & D). In MRV, the joining of this domain from the five subunits in each turret leads to the formation of a central cavity, which is thought to allow passage of the nascent viral plus-strand RNAs as they undergo 5'-capping and are released from the transcribing viral particle.[13; 32]

The outer capsid hexon -- VP5-VP7 complex

The outer capsid of GCRV is composed of 200 trimers of VP5-VP7 heterodimers (Fig. 2D and 2F). Three copies of the finger-like VP7 stack upon three copies of VP5 forming a VP5-VP7 complex, a structure homologous to the $\mu1_3\sigma3_3$ complex of MRV. In contrast to the high level of structural similarities observed on the inner capsid protein VP3, the GCRV VP5-VP7 complex exhibits pronounced structural differences from its structural homolog of MRV. More specifically, while the crystal structure of μ1 fits well with VP5, σ3 structure does not fit at all in the cryoEM density of GCRV VP7 (Fig. 4).

Interactions between inner and outer capsids mediated by clamping protein, VP6

A total of 120 VP6 molecules, a homolog of MRV σ2 or CPV LPP, clamp and secure the VP3 inner capsid shell (Fig. 2A and Fig. 5A, B).[11] Notably, this is similar to the situation of CPV, but different from MRV or ARV core, where 150 nodules are found,[26] including 30 nodules at the twofold vertices, which are unoccupied in the GCRV core and CPV. Like LPP in CPV, there are two conformers of VP6 located at two different positions in an asymmetric unit: VP6A surrounding each fivefold axis and VP6B surrounding each threefold axis. Although VP6A and VP6B are roughly identical in their structures, they have different interaction modes with the underlying VP3 molecules (Fig. 5B). Similar to related interactions of CPV, each VP6A interacts with one copy of VP3A and VP3B; whereas each VP6B contacts one copy of VP3A and two copies of VP3B (Fig. 5B). Having an outer shell, the GCRV VP6 has an additional role as a mediator bridging the inner core with the outer shell (Fig. 5C–D). VP6A also has a weak interaction with turret protein VP1 (Fig. 5D).

The availability of the 3D structures of both the GCRV inner core and intact virion presented here makes it possible to more precisely dissect the interactions between the proteins located on the outer shell and those on the core. These interactions involve outer capsid protein VP5 with inner capsid proteins VP6 and VP1. There are four kinds of contact modes among these proteins (Fig. 5C–D). The four types of trimers (VP5-VP7) have four different interaction modes with the clamping protein VP6. As shown in Fig. 5D, Trimer 1 has one copy of VP5 interacting with both VP6A and VP1; Trimer 2 has only one copy of VP5 interacting with VP6A; Trimer 3 has two copies of VP5 interacting with VP6A and VP6B respectively; Trimer 4 has three copies of VP5 interacting with three copies of VP6B respectively. These interactions between the mediator VP6 and VP5-VP7 trimers are tenuous as judged by the small contact areas (Fig. 5D), which accords well with our experimental observation that the GCRV outer shell was readily removed from inner core (data not shown). Such loose interactions can facilitate the process of VP5-VP7 detachment prior to endogenous RNA transcription in the cytoplasm during early stage of viral replication.

Discussion

Within the *Reoviridae* family, the cores of the “turreted viruses” group – including aquareoviruses, orthoreoviruses and cypoviruses – are distinguished from those in the “smooth viruses” group – including the BTV,[33] RDV,[30] and rotaviruses – in having decorated elements on the core shell. This difference at the viral architecture or structural organization reflects the first level of divergence within the family of *Reoviridae*.

GCRV core is composed of 5 proteins:[19] VP1, VP2, VP3, VP4 and VP6. Comparing the protein homologs in GCRV to MRV, the levels of protein sequence similarity exhibit a decreasing trend from the inner capsid proteins toward the outer capsid proteins (Table 1). Interestingly, VP6, the clamping protein located at the intermediate layer, exhibits some obvious divergence across the turreted virus genera of the *Reoviridae*. GCRV contains 120 copies of VP6, rather than the 150 copies of σ2 of orthoreovirus with three conformers. This organization of the clamping protein on the GCRV core is similar to that in CPV of the cypovirus genus, whose members are the structurally simplest among the *Reoviridae*, with only a single protein shell [18; 23].

Of particular note is that GCRV lacks the MRV protein σ1 counterpart, which functions as the cell attachment protein situated on each fivefold vertex. Comparing VP1 to its MRV homolog reveals a similar overall topological structure and conserved domains involved in RNA post-transcription processing at the pentameric core turret. There are three immunoglobulin-like flap domains located at the distal end of MRV VP1, which are all believed to be involved in regulating the release of capped transcripts.[13; 32; 34; 35] In MRV virions and its infectious

subviral particles (ISVP), the residues in the most carboxyl-(C-) terminal immunoglobulin-like flap domain probably contact the base of the σ1 receptor-binding domain in virions.[13; 32; 36] In this case, these residues may contribute to the σ1 anchoring to λ2.36 Since no σ1 structural analog has been found in GCRV, we postulate that the VP1 flap domains might also be involved in conferring host specificity during virus entry into cells.

Amongst all the homologous structural proteins between GCRV and MRV, VP7 shares the lowest sequence identity with its counterpart σ3 of MRV, with a sequence identity of only 12%, which is close to the identity level between random protein sequences (Table 1). This identity is also much lower than the 24% identity between VP5 and μ1. Indeed, VP5 and μ1 appear to share a very similar overall structure (Fig. 4A). Both domains μ1N (red spheres) and μ1C (gray ribbon) fit well in our cryoEM density map (semi-transparent surface view in Fig. 4B), suggesting GCRV VP5 and MRV μ1 have similar functional roles. In fact, the N-terminal region up to the autolytic cleavage site (Asn42-Pro43) is highly conserved with that of μ1, pointing to a similar myristoyl switch mechanism employed by VP5 for membrane penetration as by μ1 during virus entry into host cells. However, cell entry is a complex process and involves one more protein. The low sequence identity between VP7 and MRV σ3 indicates that they have acquired very divergent sequence segments in the course of evolving distinct patterns of virus-cell interaction. In MRV, σ3 plays critical roles in μ1 assembly into progeny particles by protecting μ1 and regulating the conformational status in order to expose μ1 for engaging in membrane penetration.[28] VP7 likely plays similar roles in cell attachment and may also be involved in signal transduction to help host recognition and attachment.

In summary, the structural similarities and differences between GCRV and other *Reoviruses* may represent species- and genus-specific divergence related to viral host interactions. Our study revealed a high level of structural similarities between GCRV and MRV in their inner capsid shells. The conserved structures are largely those functional and enzymatic domains which are responsible for maintaining inner core shell stability and endogenous transcription activity. Beyond the conserved inner capsid shell proteins, however, intermediate (e.g., clamping protein VP6) and outer protein components of these dsRNA viruses have significantly diverged. Outer capsid proteins are involved directly in viral-host interactions and clearly exhibit an even greater level of divergence. For example, in CPV, there are A spikes which sit atop the turret [22]. In rotavirus, VP4 cell attachment proteins insert into the P2 channels 37. MRV has a cell attachment protein σ1 38; 39. However, GCRV has no homolog of such a cell attachment protein, pointing to a different mechanism of attachment. These complexities in viral protein conservation and diversification clearly support the notion that aquareoviruses occupies a unique position across different genera of the *Reoviridae*.

Materials and Methods

Cell culture and viral growth

CIK (*Ctenopharyngodon idellus* kidney) cells were grown as monolayer at 28°C in Eagle's minimum essential medium (MEM, Gibco) supplemented with fetal bovine serum (10%, FBS), and penicillin (100 U/ml)-streptomycin(100 mg/ml) (Sigma). GCRV was propagated in CIK cell cultures grown in 50cm^2 flasks (Corning). Confluent monolayer of cells was infected with a virus stock at about 5–10 PFU/ml MOI (multiplicity of infection). The infected cells were overlaid with maintenance medium (MEM) containing only 2% FBS (MEM-2) and incubated for 3 days at 28°C until mature virions released almost completely from infected cells.[10] Collected GCRV culture suspension was stored at −20°C for further use.

Purification of GCRV Virions and cores

GCRV particles were recovered from the infected cell-culture supernatants by extraction with different low speed centrifugation to get rid of cell debris, ultracentrifugation to pellet virus, and purification on sucrose density gradients to isolate uniform particles, as described elsewhere.[19] The cores of GCRV were obtained by treating purified virions in vitro with 200μg/ml a-chymotrypsin (Sigma). The treatment occurred in 10mM PBS buffer at 37°C for 2 h. The resulting cores were further purified by banding on 20~50% CsCl (ρ=1.25 to 1.50 g/cm^3) gradient. A sharp band was clearly visible in the gradient and was collected and checked through negative stained transmission electron microscopy to confirm the presence of highly purified virus core. Both purified cores and intact particles collected from gradients were dialyzed against 10mM PBS and stored at −20°C until use.

CryoEM

Specimen preparation for cryoEM was carried out using conventional procedures. Gradient-purified GCRV virions/cores were quickly plunged into a bath of liquid ethane cooled by liquid nitrogen. The GCRV cores and virions were imaged using FEI 300 kV G2 Polara transmission electron microscope equipped with TVIPS 16-megapixel CCD. The cores were imaged at 200 kV with a magnification of 78,000×, corresponding to 1.16 Å pixel size. The virions were imaged at 300 kV with a magnification of 93,000×, corresponding to 0.97 Å pixel size. For both the core and the virion, focal pair images were recorded at under focus values of about 1.0 μm and 2.5 μm, respectively for the close-to-focus and far-from-focus images.

3D reconstruction and visualization

Image processing and 3D reconstruction was performed with our established procedure[40] using the IMIRS software package[41] on a Dell Workstation running Microsoft Windows XP. Orientation estimation and refinement were done using both Fourier common-line[42]; 43 and projection matching44 methods. 3D reconstruction were performed first by Fourier-Bessel synthesis45 and subsequently by spherical harmonics methods.[46] The defocus values of images were estimated from the positions of the contrast transfer function (CTF) rings visible in the incoherently averaged Fourier transforms of particle images,[47] using ctfit program of the EMAN package.48 CTF correction and B factor compensation were performed as previously described.49 The focal-pair approach of orientation estimation was used; i.e., the orientation parameters were first determined from the far-from-focus pictures of the focal pairs and subsequently refined to higher resolution using the close-to-focus pictures.40 Only the close-to-focus particle images were included in the final 3D reconstruction. Some particle images were eliminated based on phase residual and cross-correlation evaluations during orientation refinement and only 85% and 70% of the initially selected particle images were included in the final core and virion reconstructions, respectively.

The structures were segmented, displayed and fitted with MRV crystal structures using UCSF Chimera.[50] We optimized the fitting by using the “Fit Model in Map” function of chimera (Tools->Volume Data->Fit Model in Map), which employs a steepest ascent algorithm. During this fitting, each individual MRV protein subunit was treated as a rigid body. The molecular boundaries were defined by difference mapping of the full and core structures, by interactively assessing the continuity of the density maps at relatively higher contour levels and by comparing protein structures at quasi-equivalent positions. In addition, the well fitted crystal structures of MRV λ1[13] into our GCRV core density map provided helpful guidance for the identification of molecular boundaries.

Supplementary Material

Refer to Web version on PubMed Central for supplementary material.

Acknowledgments

We thank Ms. Xiaorui Zhang for help in graphics and editorial assistance. This research was supported in part by grants from National Institutes of Health (GM071940), the Welch Foundation (AU1409), the National Science Foundation (NSF HRD-0420407), National Natural Scientific Foundation of China (Grant Nos.30470074, 30671615 to QF) and innovation project of the Chinese Academy of Sciences (Grant No.KSCX2-YW-N-021 to QF).

References

1. Mertens P. The dsRNA viruses. Virus Res 2004;101:3–13. [PubMed: 15010213]
2. Patton, JT. Segmented Double-Stranded RNA Viruses: Structure and Molecular Biology. Norfolk, UK: Caister Academic Press; 2008.
3. van Regenmortel, MHV.; Fauquet, CM.; Bishop, DHL.; Carstens, EB.; Estes, MK.; Lemon, SM.; Maniloff, J.; Mayo, MA.; McGeoch, DJ.; Pringle, CR.; Wickner, RB. Virus Taxonomy - Seventh Report of the International Committee on Taxonomy of Viruses. San Diego, California, USA: Academic Press; 2000.
4. Lupiani B, Subramanian K, Samal SK. Aquareoviruses. Annual Review of Fish Diseases 1995;5:175–208.
5. Rangel AA, Rockemann DD, Hetrick FM, Samal SK. Identification of grass carp haemorrhage virus as a new genogroup of aquareovirus. J Gen Virol 1999;80(Pt 9):2399–2402. [PubMed: 10501493]
6. Mertens, PPC.; Arella, M.; Attoui, H.; Belloncik, S.; Bergoin, M.; Boccardo, G.; Booth, TF.; Chiu, W.; Diprose, JM.; Duncan, R.; Estes, MK.; Gorziglia, M.; Gouet, P.; Gould, AR.; Grimes, JM.; Hewat, E.; Homes, IA.; Hosshino, Y.; Hill, C.; Joklik, WK.; Knowles, N.; Ferber, ML.; Malby, R.; Marcachi, C.; McCrae, MA.; Milne, RG.; Nibert, M.; Nunn, M.; Omura, T.; Prasad, BVV.; Pritchard, I.; Roy, P.; Samal, SK.; Schoehn, G.; Shikata, E.; Stoltz, DB.; Stuart, DI.; Suzuki, N.; Upadhyaya, N.; Uyeda, I.; Waterhouse, P.; Williams, CF.; Winton, JR.; Zhou, ZH. Family Reoviridae. In: van Regenmortel, MHV.; Fauguet, CM.; Bishop, DHL.; Carstens, EB.; Estes, MK.; Lemon, SM.; Maniloff, J.; Mayo, MA.; McGeoch, DJ.; Pringle, CR.; Wickner, RB., editors. Virus Taxonomy. San Diego, CA, USA: Academic Press; 2000. p. 395-480.
7. Ke LHFQ, Cai Y-Q. Characteristics of a novel isolate of grass carp Hemorrhage Virus (In Chinese). Acta hydrobiology sinica 1990;14:153–159.
8. Fang Q, Ke L-HCY-Q. Growth characterization and high titre culture of GCHV (In Chinese). Virologica Sinica 1989;3:314–319.
9. Ke L-H, Fang Q, Yu L-F, Cai Y-Q. Sderological identification of Grass Carp Hemorrhage Virus (In Chinese). Virologica Sinica 1991;6:252–255.
10. Fang Q, Attoui H, Cantaloube JF, Biagini P, Zhu Z, de Micco P, de Lamballerie X. Sequence of genome segments 1, 2, and 3 of the grass carp reovirus (Genus Aquareovirus, family Reoviridae). Biochem Biophys Res Commun 2000;274:762–766. [PubMed: 10924351]
11. Nason EL, Samal SK, Venkataram Prasad BV. Trypsin-induced structural transformation in aquareovirus. J Virol 2000;74:6546–6555. [PubMed: 10864668]
12. Attoui H, Fang Q, Mohd Jaafar F, Cantaloube JF, Biagini P, de Micco P, de Lamballerie X. Common evolutionary origin of aquareoviruses and orthoreoviruses revealed by genome characterization of Golden shiner reovirus, Grass carp reovirus, Striped bass reovirus and golden ide reovirus (genus Aquareovirus, family Reoviridae). J Gen Virol 2002;83:1941–1951. [PubMed: 12124458]
13. Reinisch KM, Nibert ML, Harrison SC. Structure of the reovirus core at 3.6 Å resolution. Nature 2000;404:960–967. [PubMed: 10801118]
14. Zhang X, Walker SB, Chipman PR, Nibert ML, Baker TS. Reovirus polymerase lambda 3 localized by cryo-electron microscopy of virions at a resolution of 7.6 A. Nat Struct Biol 2003;10:1011–1018. [PubMed: 14608373]
15. Zhang X, Ji Y, Zhang L, Harrison SC, Marinescu DC, Nibert ML, Baker TS. Features of reovirus outer capsid protein mu1 revealed by electron cryomicroscopy and image reconstruction of the virion at 7.0 Angstrom resolution. Structure 2005;13:1545–1557. [PubMed: 16216585]
16. Estes MK. Rotaviruses and their replication. Virology 1990:1353–1404.
17. Grimes JM, Burroughs JN, Gouet P, Diprose JM, Malby R, Zientara S, Mertens PPC, Stuart DI. The atomic structure of the bluetongue virus core. Nature 1998;395:470–478. [PubMed: 9774103]

18. Zhou ZH, Zhang H, Jakana J, Lu X-Y, Zhang J-Q. Cytoplasmic polyhedrosis virus structure at 8 Å by electron cryomicroscopy: structural basis of capsid stability and mRNA processing regulation. Structure 2003;11:651–663. [PubMed: 12791254]
19. Fang Q, Shah S, Liang Y, Zhou ZH. 3D reconstruction and capsid protein characterization of grass carp reovirus. Sci China C Life Sci 2005;48:593–600. [PubMed: 16483138]
20. Shaw AL, Samal SK, Subramanian K, Prasad BV. The structure of aquareovirus shows how the different geometries of the two layers of the capsid are reconciled to provide symmetrical interactions and stabilization. Structure 1996;4:957–967. [PubMed: 8805574]
21. Kim J, Tao Y, Reinisch KM, Harrison SC, Nibert ML. Orthoreovirus and Aquareovirus core proteins: conserved enzymatic surfaces, but not protein-protein interfaces. Virus Res 2004;101:15–28. [PubMed: 15010214]
22. Zhang H, Zhang J, Yu X, Lu X, Zhang Q, Jakana J, Chen DH, Zhang X, Zhou ZH. Visualization of protein-RNA interactions in cytoplasmic polyhedrosis virus. J Virol 1999;73:1624–1629. [PubMed: 9882369]
23. Hill CL, Booth TF, Prasad BV, Grimes JM, Mertens PP, Sutton GC, Stuart DI. The structure of a cypovirus and the functional organization of dsRNA viruses. Nat Struct Biol 1999;6:565–568. [PubMed: 10360362]
24. Zhou, ZH. Cypovirus. In: Patton, JT., editor. Segmented Double-Stranded RNA Viruses: Structure and Molecular Biology. Norfolk, UK: Caister Academic Press; 2008. p. 27-43.
25. Xia Q, Jakana J, Zhang JQ, Zhou ZH. Structural comparisons of empty and full cytoplasmic polyhedrosis virus: protein-RNA interactions and implications for endogenous RNA transcription mechanism. J Biol Chem 2003;278:1094–1100. [PubMed: 12401805]
26. Zhang X, Tang J, Walker SB, O'Hara D, Nibert ML, Duncan R, Baker TS. Structure of avian orthoreovirus virion by electron cryomicroscopy and image reconstruction. Virology 2005;343:25–35. [PubMed: 16153672]
27. Nibert ML. Structure of mammalian orthoreovirus particles. Curr Top Microbiol Immunol 1998;233:1–30. [PubMed: 9599919]
28. Liemann S, Chandran K, Baker TS, Nibert ML, Harrison SC. Structure of the reovirus membrane-penetration protein, Mu1, in a complex with is protector protein, Sigma3. Cell 2002;108:283–295. [PubMed: 11832217]
29. Shaw AL, Rothnagel R, Chen D, Ramig RF, Chiu W, Prasad BVV. Three-dimensional visualization of the rotavirus hemagglutinin structure. Cell 1993;74:693–701. [PubMed: 8395350]
30. Zhou ZH, Baker ML, Jiang W, Dougherty M, Jakana J, Dong G, Lu G, Chiu W. Electron cryomicroscopy and bioinformatics suggest protein fold models for rice dwarf virus. Nat Struct Biol 2001;8:868–873. [PubMed: 11573092]
31. Qiu T, Luongo CL. Identification of two histidines necessary for reovirus mRNA guanylyltransferase activity. Virology 2003;316:313–324. [PubMed: 14644613]
32. Dryden KA, Wang GJ, Yeager M, Nibert ML, Coombs KM, Furlong DB, Fields BN, Baker TS. Early steps in reovirus infection are associated with dramatic changes in supramolecular structure and protein conformations. J. Cell Biol 1993;122:1023–1041. [PubMed: 8394844]
33. Hewat EA, Booth TF, Loudon PT, Roy P. Three-dimensional reconstruction of baculovirus expressed bluetongue virus core-like particles by cryo-electron microscopy. Virology 1992;189:10–20. [PubMed: 1318601]
34. Bartlett N, Gillies S, Bullivant S, Bellamy A. Electron microscopy study of reovirus reaction cores. Journal of Virology 1974;14:315–326. [PubMed: 4136229]
35. Yeager MWS, Coombs KM. Transcriptionally active reovirus core particles visualized by electron cryo-microscopy and image reconstruction. Biophysical Journal 1996;70:A116.
36. Chandran K, Zhang X, Olson NH, Walker SB, Chappell JD, Dermody TS, Baker TS, Nibert ML. Complete in vitro assembly of the reovirus outer capsid produces highly infectious particles suitable for genetic studies of the receptor-binding protein. J Virol 2001;75:5335–5342. [PubMed: 11333914]
37. Prasad BVV, Burns JW, Marietta E, Estes MK, Chiu W. Localization of VP4 neutralization sites in rotavirus by three-dimensional cryo-electron microscopy. Nature (London) 1990;343:476–479. [PubMed: 2153941]

38. Chappell JD, Prota AE, Dermody TS, Stehle T. Crystal structure of reovirus attachment protein sigma1 reveals evolutionary relationship to adenovirus fiber. Embo J 2002;21:1–11. [PubMed: 11782420]
39. Nibert ML, Chappell JD, Dermody TS. Infectious subvirion particles of reovirus type 3 Dearing exhibit a loss in infectivity and contain a cleaved sigma 1 protein. J Virol 1995;69:5057–5067. [PubMed: 7609075]
40. Zhou ZH, Chiu W. Determination of icosahedral virus structures by electron cryomicroscopy at subnanometer resolution. Advances in Protein Chemistry 2003;64:93–124. [PubMed: 13677046]
41. Liang Y, Ke EY, Zhou ZH. IMIRS: a high-resolution 3D reconstruction package integrated with a relational image database. J Struct Biol 2002;137:292–304. [PubMed: 12096897]
42. Fuller SD, Butcher SJ, Cheng RH, Baker TS. Three-dimensional reconstruction of icosahedral particles--the uncommon line. J Struct Biol 1996;116:48–55. [PubMed: 8742722]
43. Crowther RA, DeRosier DJ, Klug A. The reconstruction of a three-dimensional structure from projections and its application to electron microscopy. Proc. Roy. Soc. London 1970;317:319–340.
44. Baker TS, Cheng RH. A model-based approach for determining orientations of biological macromolecules imaged by cryoelectron microscopy. J. Struct. Biol 1996;116:120–130. [PubMed: 8742733]
45. Crowther RA, Amos LA, Finch JT, DeRosier DJ, Klug A. Three dimensional reconstructions of spherical viruses by Fourier synthesis from electron micrographs. Nature 1970;226:421–425. [PubMed: 4314822]
46. Liu H, Cheng L, Zeng S, Cai C, Zhou ZH, Yang Q. Symmetry-adapted spherical harmonics method for high-resolution 3D single-particle reconstructions. J Struct Biol 2008;161:64–73. [PubMed: 17977017]
47. Zhou ZH, Hardt S, Wang B, Sherman MB, Jakana J, Chiu W. CTF determination of images of ice-embedded single particles using a graphics interface. J Struct Biol 1996;116:216–222. [PubMed: 8742746]
48. Ludtke SJ, Baldwin PR, Chiu W. EMAN: Semi-automated software for high resolution single particle reconstructions. J Struct Biol 1999;128:82–97. [PubMed: 10600563]
49. Zhou ZH, Chen DH, Jakana J, Rixon FJ, Chiu W. Visualization of tegument-capsid interactions and DNA in intact herpes simplex virus type 1 virions. J Virol 1999;73:3210–3218. [PubMed: 10074174]
50. Pettersen EF, Goddard TD, Huang CC, Couch GS, Greenblatt DM, Meng EC, Ferrin TE. UCSF Chimera--a visualization system for exploratory research and analysis. J Comput Chem 2004;25:1605–1612. [PubMed: 15264254]

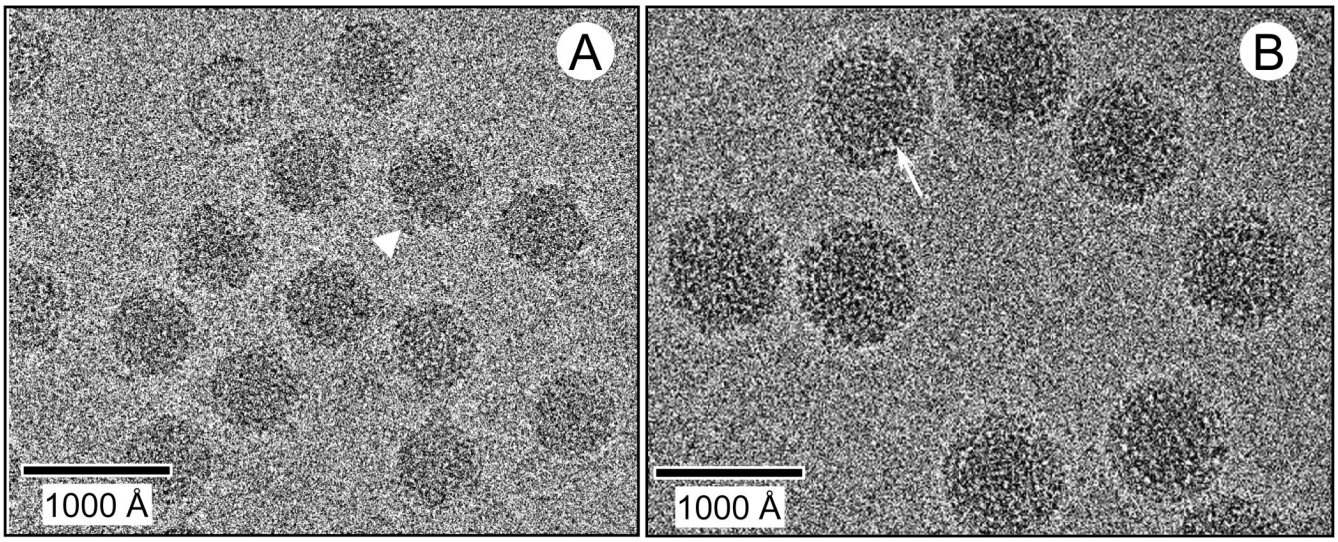

Fig. 1. CryoEM images of GCRV particles

(A) GCRV cores. Arrowhead indicates a turret. (B) GCRV virion. Arrow points to an electron-lucent boundary between inner and outer layers.

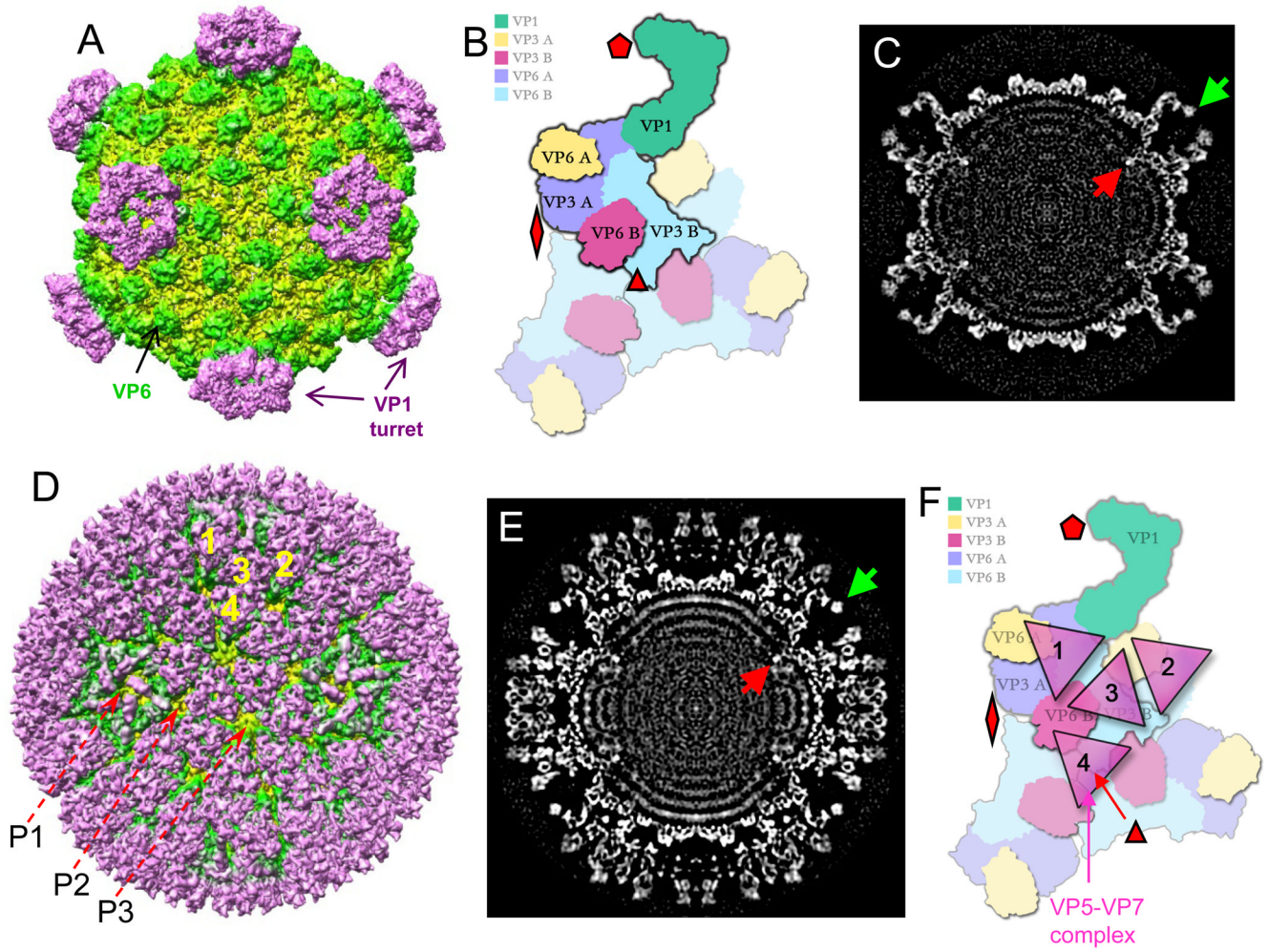

Fig. 2. Structural representation of GCRV core and virion

(A) Radially coloured shaded surface representation of GCRV core viewed along twofold axis. The VP6 nodules are in green and the VP1 turrets are in purple. (B) A cartoon illustrating the protein organization in an asymmetric unit (in darker colours) and their symmetry-related proteins (in lighter colours). (C) A central slice from (A). A transcriptase complex under a fivefold vertex is indicated by a red arrow. The green arrow indicates an immunoglobulin-like flap domain. (D) Radially coloured shaded surface representation of GCRV virion. Four kinds of quasi-equivalent trimers are marked by 1, 2, 3 and 4. Three types of conduits -- P1, P2 and P3 -- are also indicated. (E) A central slices of GCRV virion from (D). A transcriptase complex under a fivefold vertex is indicated by a red arrow. The green arrow indicates an immunoglobulin-like flap domain. (F) A cartoon illustrating organization of capsid proteins within three adjacent asymmetric units. Triangles represent VP5-VP7 complex on the virion.

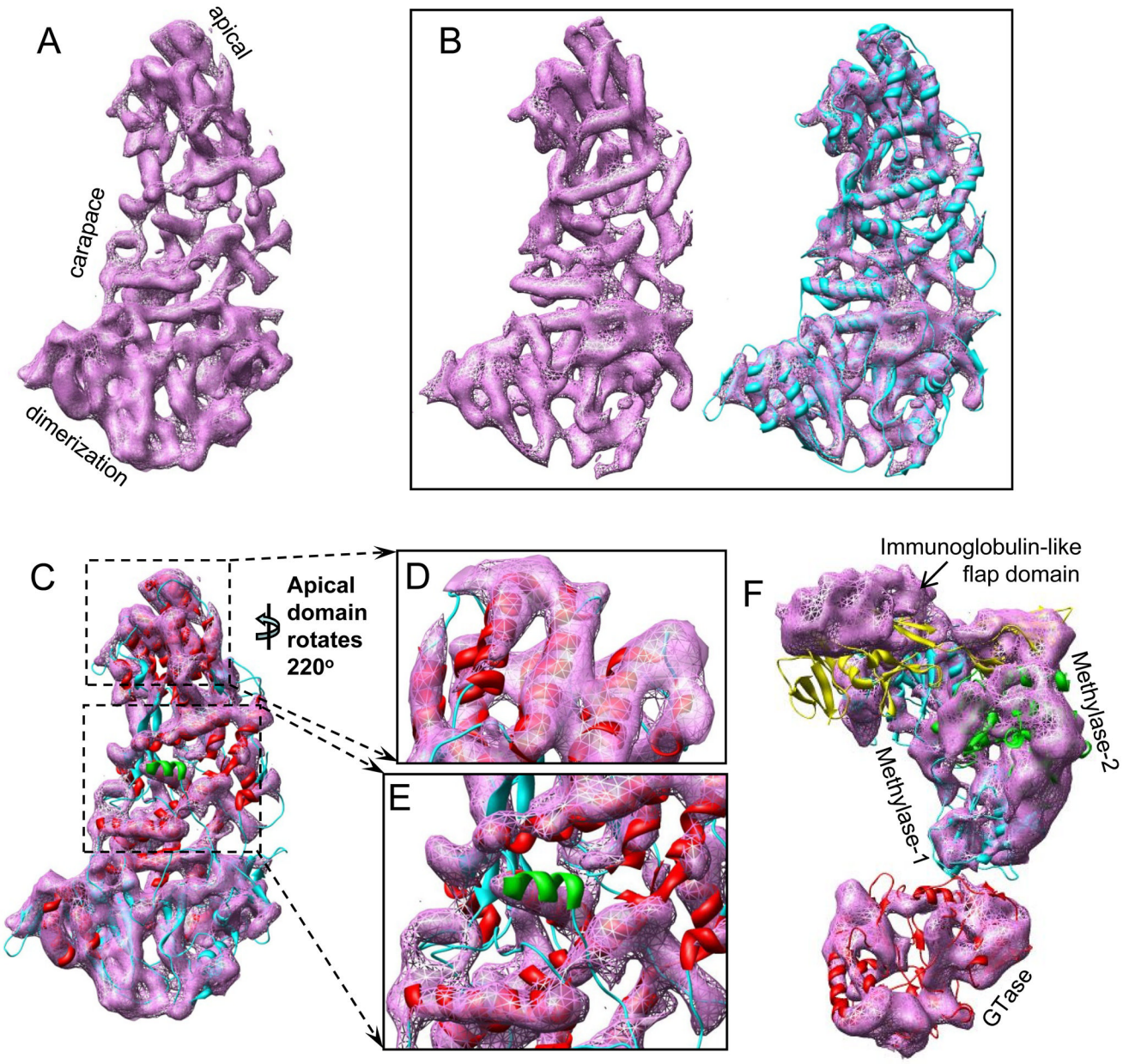

Fig. 3. VP3A and VP1

(A) VP3A segmented from density map of core capsid. (B) Simulated density map of λ1A from crystal structure of MRV core (PDB code: 1EJ6),[13] which was gaussian-filtered to 9-Å resolution (left) and superposed with its crystal structure (cyan) in ribbon (right) to delineate secondary structural elements. (C) Fitting of λ1A crystal structure of into VP3A density map of GCRV. Helices are in red, an N-terminal helix that cannot be assigned to any density of VP3A is in green, and the rest is in blue (cyan). (D) and (E) are zoom-in views of apical domain and carapace domain, respectively. (F) Fitting of MRV λ2 crystal structure (ribbon, PDB code: 1EJ6)13 into VP1 density map of GCRV with different domains shown in different colours as labelled.

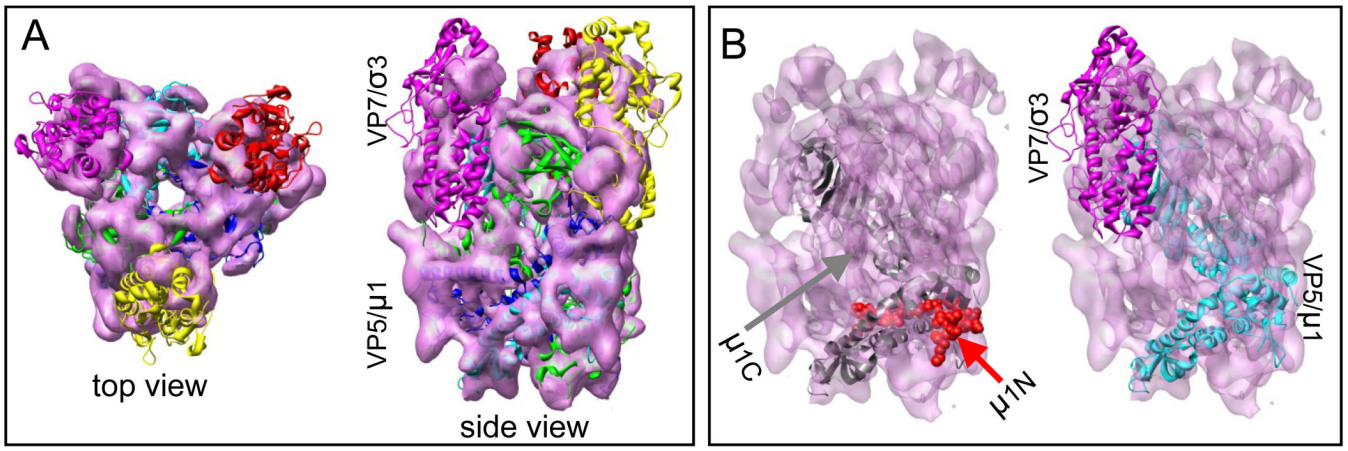

Fig. 4. Trimers of VP5-VP7 heterodimers

(A) Top view (left) and side view (right) of the superposition of GCRV VP5-VP7 trimer density map with MRV μ1σ3 atomic model (PDB code: 1JMU) [28] shown in ribbon. The three σ3 molecules are located on top and are shown in red, purple, and yellow. The three molecules of μ1 are at the bottom and are shown in blue, green, and cyan. (B) Left: the μ1N (red spheres) and μ1C (gray ribbon) atomic models are fitted into the density map of the VP5-VP7 trimer (semi-transparent purple surface). Right: the crystal structures of one μ1 (purple ribbon) and one σ3 (cyan ribbon) are fitted in our density map.

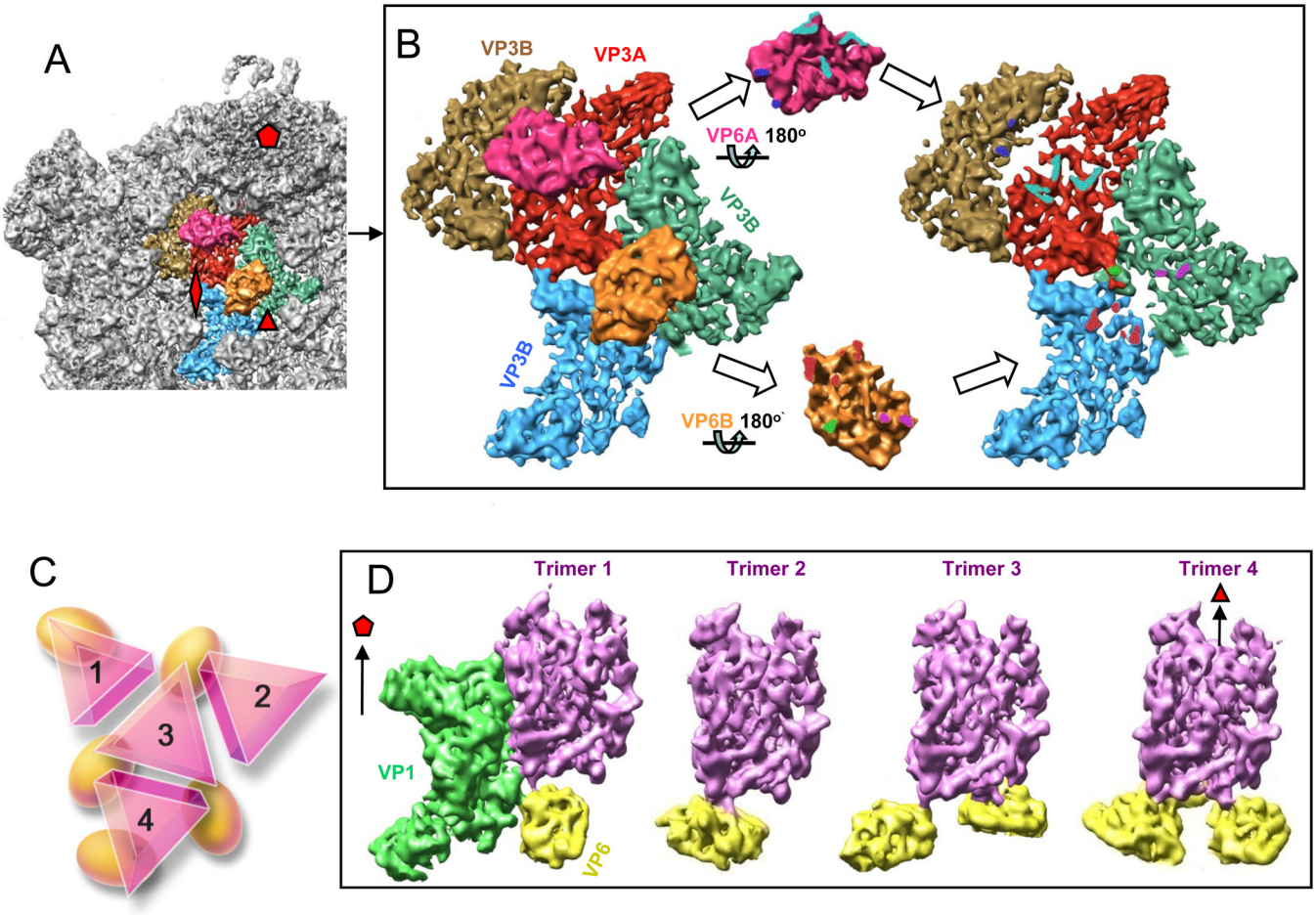

Fig. 5. Molecular interactions in GCRV virion

(A) Zoom-in view of the core with segmented parts shown in colour. (B) Interactions of VP3 and clamping protein VP6. The two right panels reveal the contact points (highlighted using a colour roughly opposite to the surface colour of the molecule of interest itself) between VP3 and VP6 by computationally rotating VP6A and VP6B away as shown. (C) Cartoon illustrating the interactions between the clamping protein VP6 (yellow) and VP5-VP7 trimers (pink, labelled 1–4) located on the outer capsid. (D) From left to right are segmented trimer 1, 2, 3 and 4 as defined in (C). Colour codes: VP1 in green, VP6 in yellow, VP5-VP7 trimer in pink. Fivefold and threefold vertices are indicated by pentagons and triangles, respectively.

Table 1

Equivalents between MRV and Aquareovirus structural proteins

Aquareovirus Protein	MRV protein	Sequence identity (%)	Sequence similarity (%)	Structural component
VP7	σ3	12.6	21.4	Outmost capsid protein
No equivalent	σ1	-	-	-
VP5	μ1	24.0	38.4	Outer capsid protein
VP6	σ2	20.3	33.1	Nodules at inner capsid
VP1	λ2	26.4	40.6	Fivefold turrets and P1 conduits
VP4	μ2	21.9	35.5	putative cofactor/nucleosi de triphosphate phosphohydrolase
VP3	λ1	30.3	45.1	Inner capsid shell protein
VP2	λ3	41.2	55.5	RNA-dependent RNA polymerase